

Imaging Spectroscopy of a Type II solar radio burst observed by LOFAR

Nicolina Chrysaphi and Eduard P. Kontar

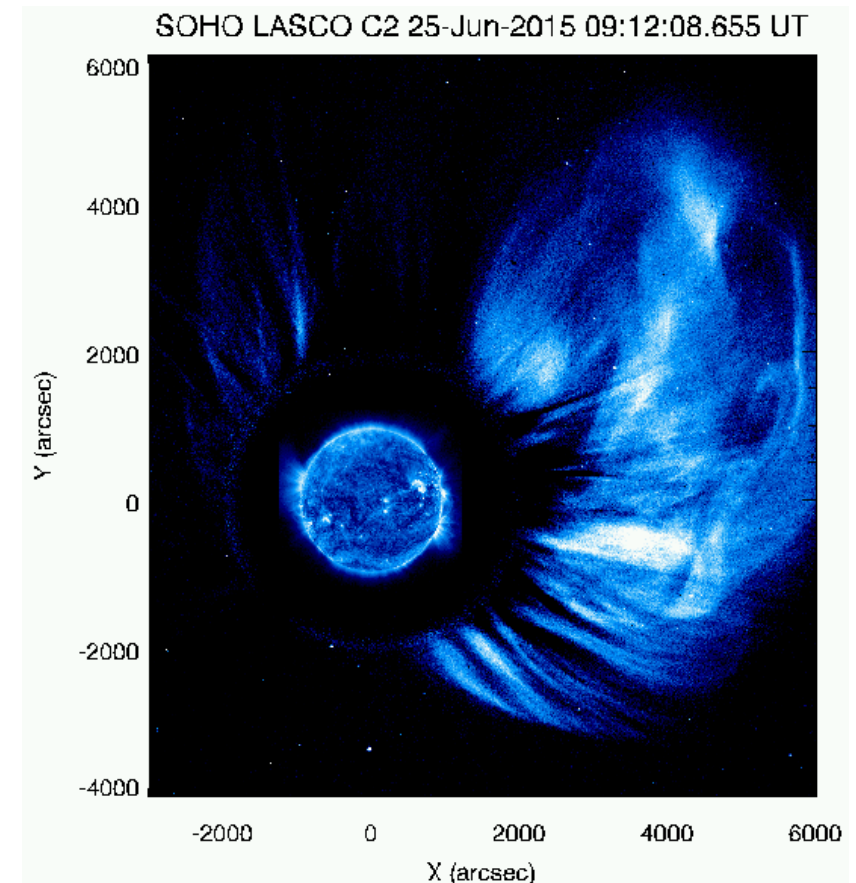
*School of Physics and Astronomy
University of Glasgow, UK*

The Broad Impact of Low Frequency Observing
20th June 2017, Bologna, Italy

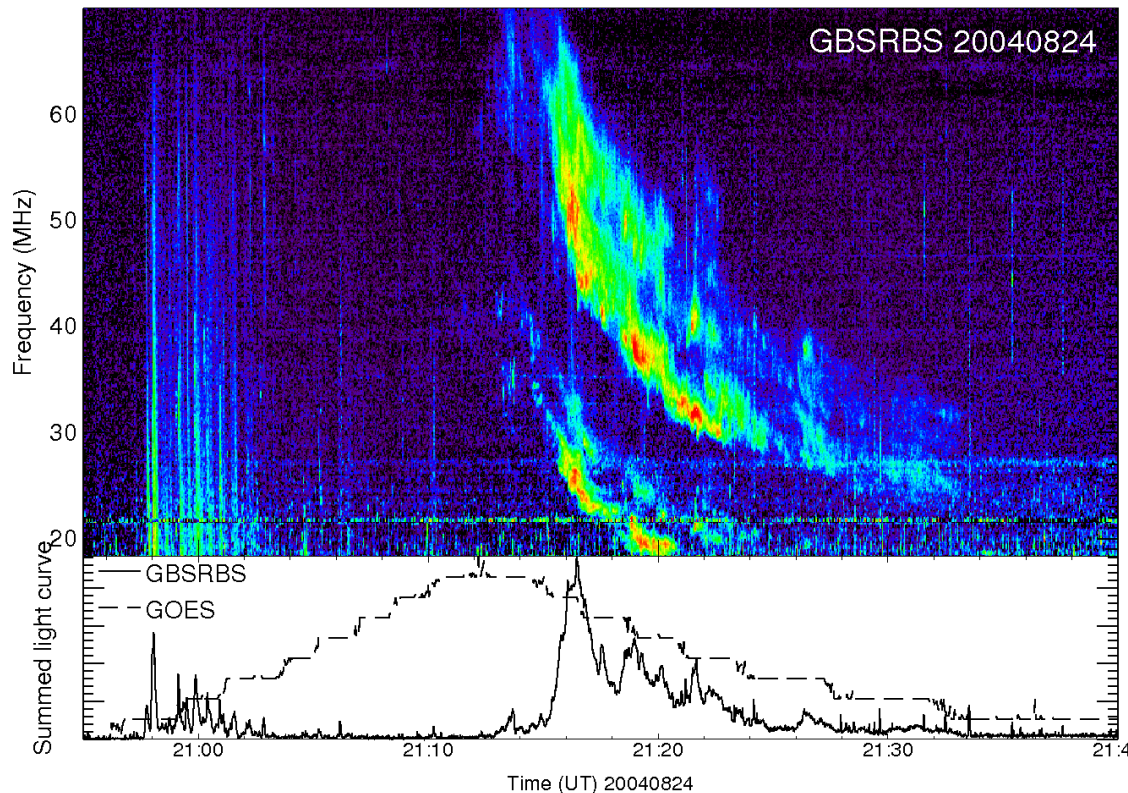


- **What are Coronal Mass Ejections and Type II solar radio bursts?**
- **Why is it important to study solar processes?**
- **How to obtain information from Type II burst observations**
 - **Using the dynamic spectrum morphology to extract the local coronal magnetic field**
 - **Imaging of the emission source**
- **Overview of obtained results**

- **Sporadic violent solar eruptions of massive plasma and magnetic structures into the interplanetary space.**
- **The rapid expulsion of particles by the CME forms abrupt discontinuities in density, pressure, and temperature producing a shock wave.**
- **A “bump-in-tail” instability in the electron beam distribution will result in Landau resonance and produce Langmuir waves. This process is referred to as the Plasma Emission mechanism.**



- Electrons excited by shock waves manifest as Type II radio bursts and radiate through the plasma emission mechanism
- Emission at fundamental (f) and second-harmonic ($2f$) of local plasma frequency can be observed (Mclean & Labrum, 1985)
- Each of the Fundamental (F) and Harmonic (H) bands can experience splitting into two thinner lanes, a phenomenon known as “**band-splitting**”

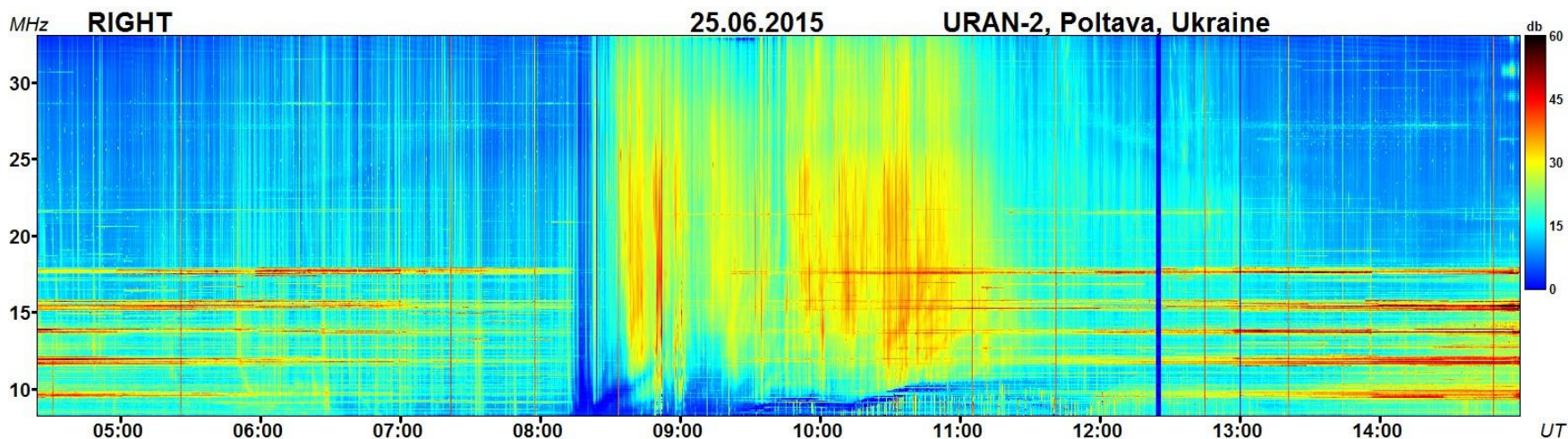


Characteristic Type II morphology due to the slow drift from high to low frequencies

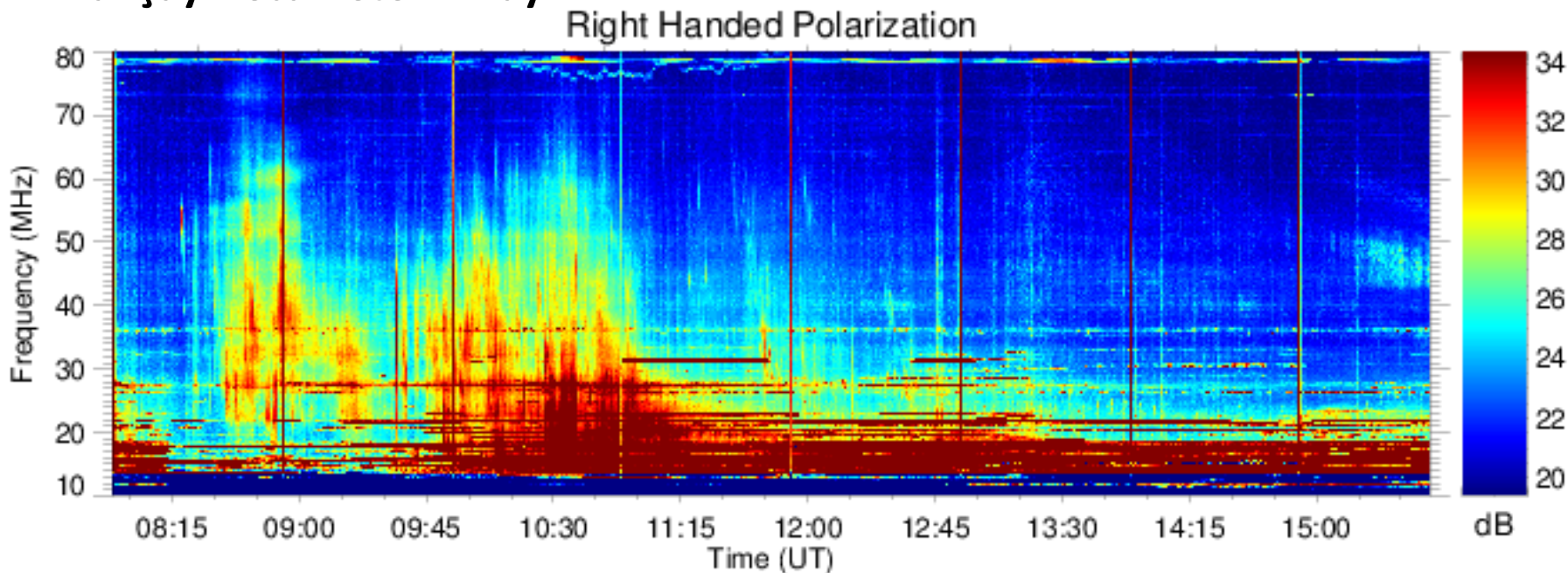
Splitting of both F and H bands is visible

- **CMEs can reach Earth and cause geomagnetic storms that can be very damaging.**
- **Type II bursts trace outward propagating shock waves and can thus be used as a diagnostic tool for shock wave parameters and local coronal conditions at each point in space.**
- **Advantage of Radio Observations: Ability to extract information from solar eruptions at distances close to the solar surface that cannot be probed in-situ or imaged at higher wavelengths.**
- **Observe the detailed structure of Type II bursts at previously largely unexplored frequencies with a telescope of unprecedented capabilities.**

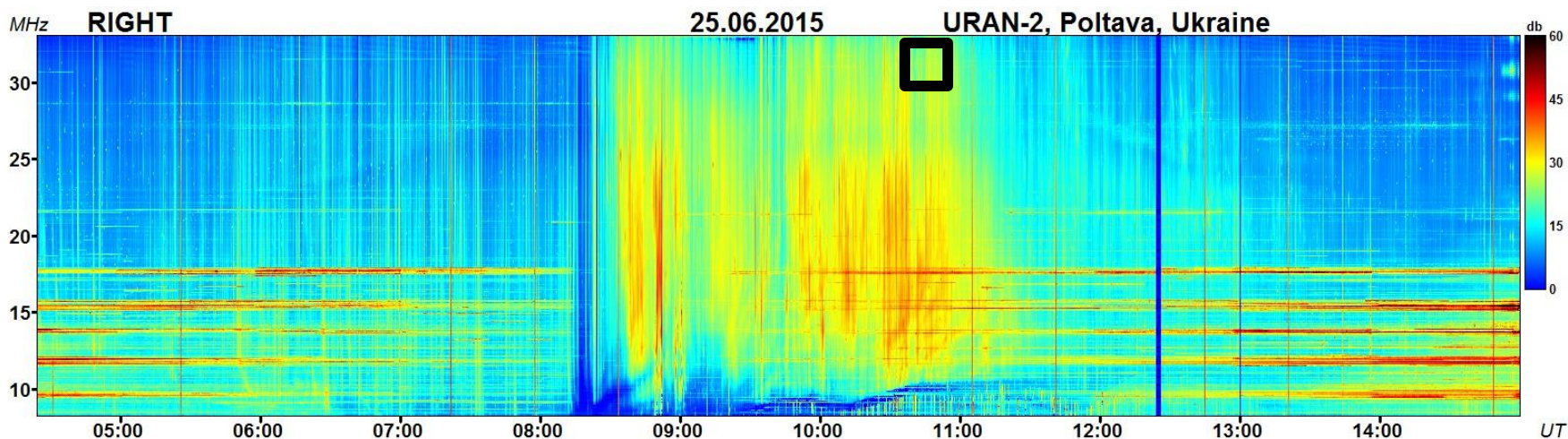
- **URAN-2**



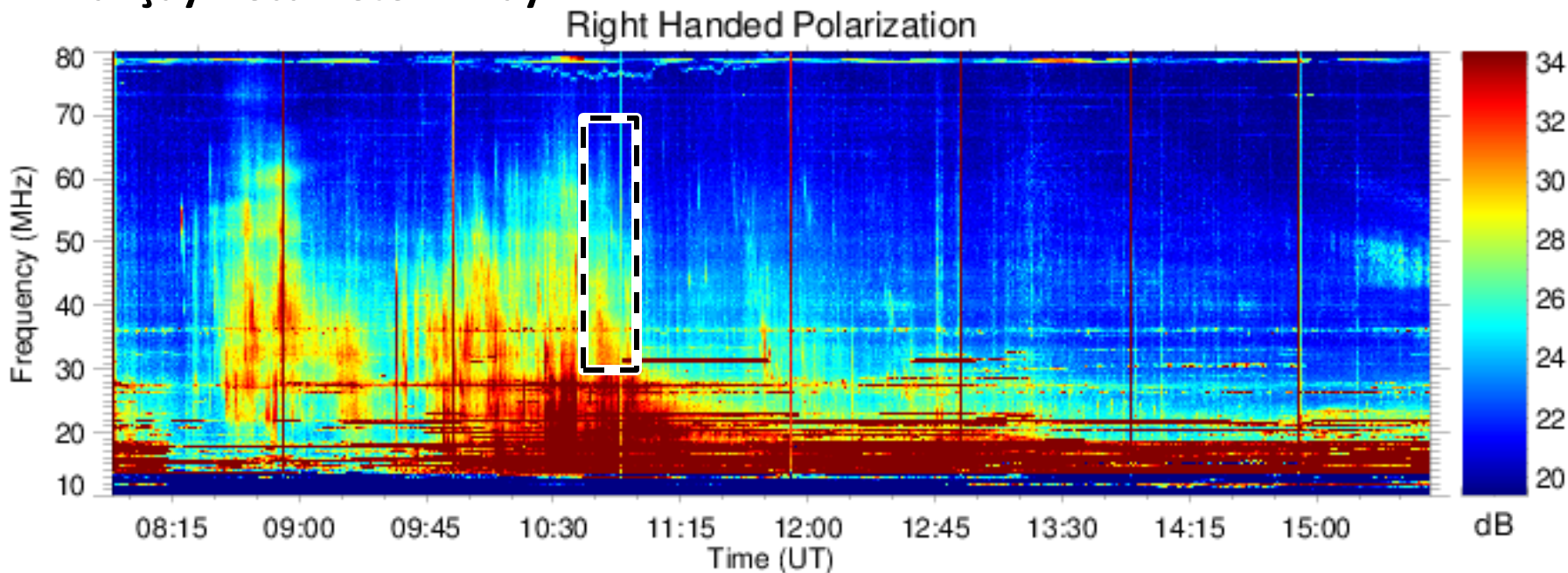
- **Nançay Decameter Array**

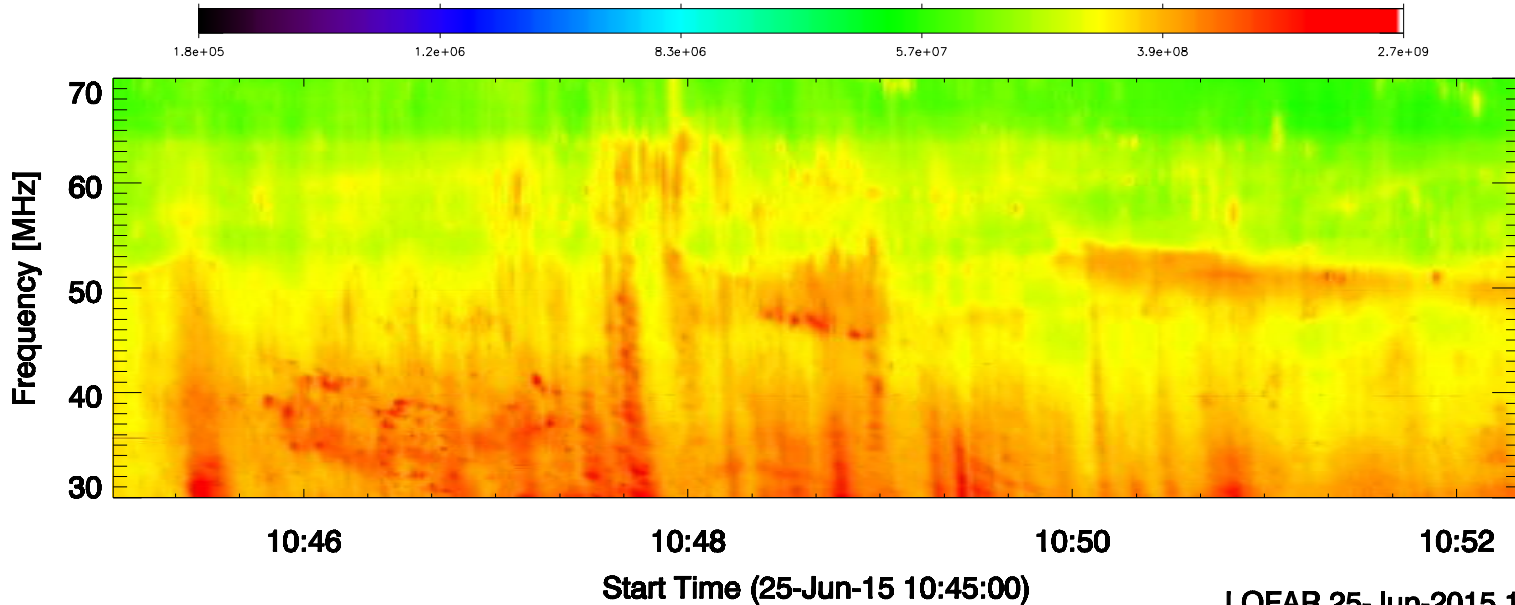


- **URAN-2**

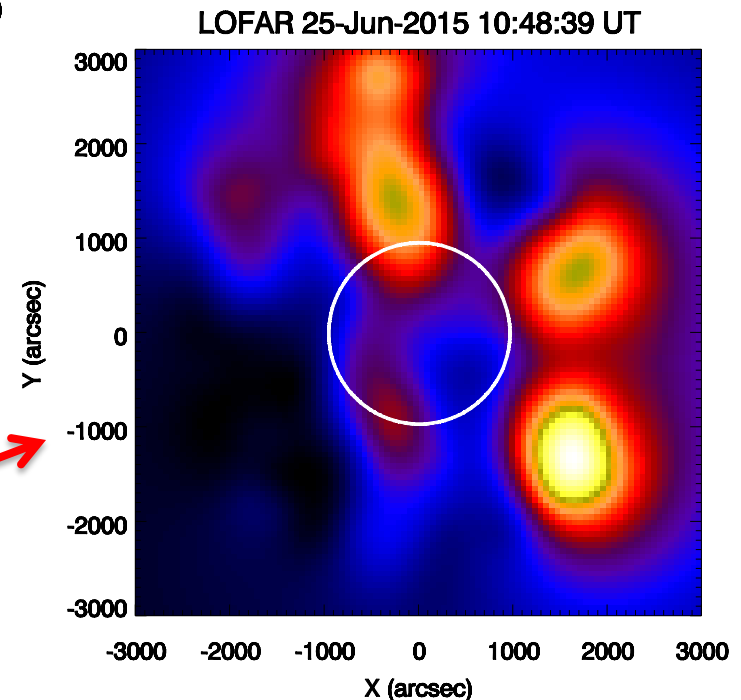


- **Nançay Decameter Array**





- Used LOFAR's LBA core stations with Coherent Stokes beam-formed mode
- Band-splitting visible between 10:46:00 and 10:47:40 UT
- Radio emission at 10:46:28 UT at about 39 MHz with respect to the solar limb (white circle)



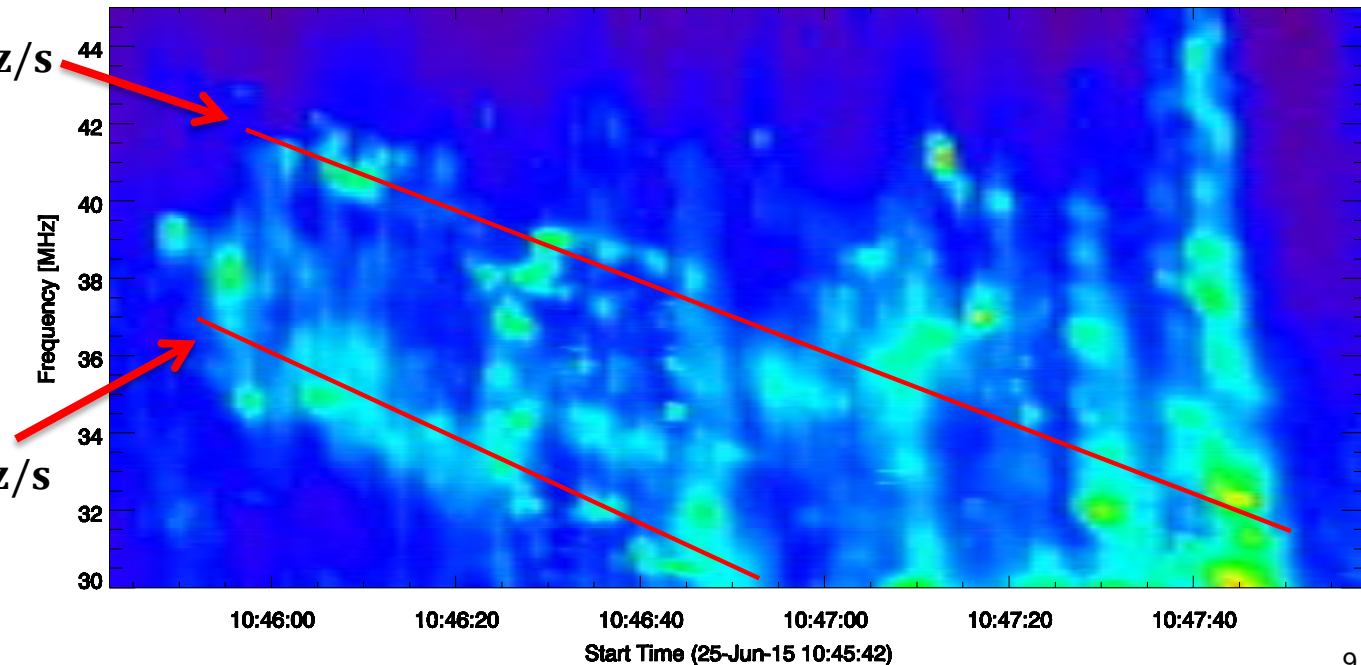
- Linear fit considering the highest intensities
- Since the band is split, a fit was applied on each of the upper and lower band parts
- Frequency drift rate given by gradient of line
- Decrease in frequency with time corresponds to decrease in densities encountered as shock propagates away from the Sun

$$\left(\frac{df}{dt}\right)_{upper}$$

$$= -0.092 \text{ MHz/s}$$

$$\left(\frac{df}{dt}\right)_{lower}$$

$$= -0.110 \text{ MHz/s}$$



- Assume fundamental emission,

$$f_{pe} = 8.98 \times 10^3 \sqrt{n_e} \quad [\text{Hz}]$$

where: n_e is in cm^{-3}

- Take the **1xNewkirk** coronal density model (1961):

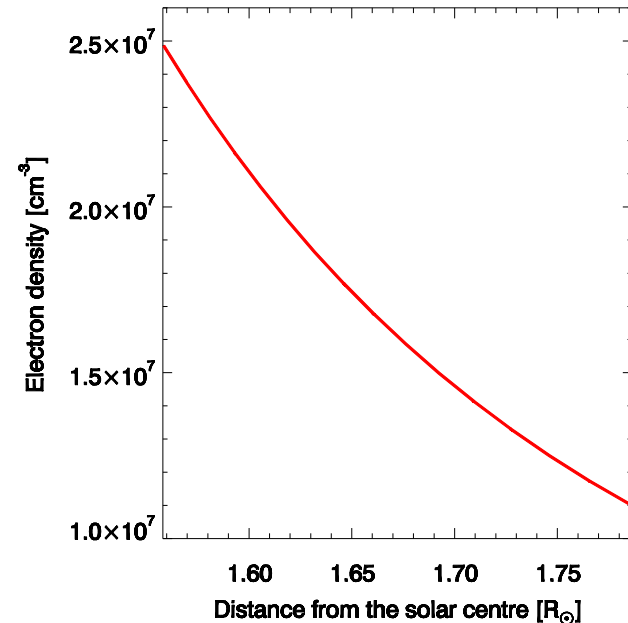
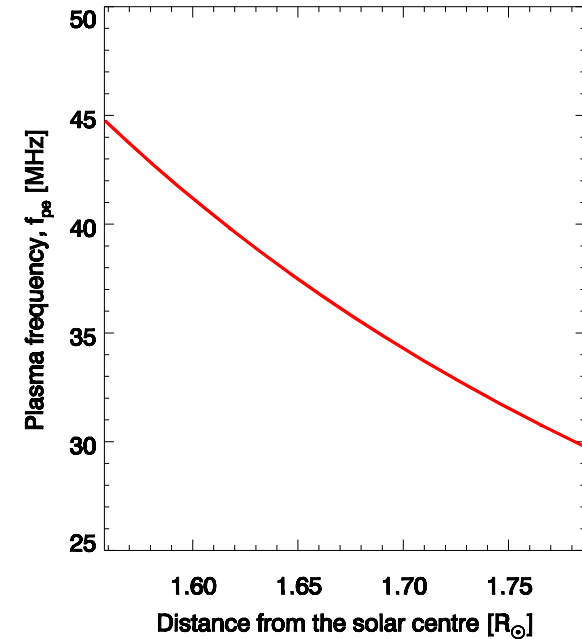
$$n_e = N \times n_0 \times 10^{4.32/R} \quad [\text{cm}^{-3}]$$

where: $n_0 = 4.2 \times 10^{10} \text{ cm}^{-3}$

$N = 1$ for 1xNewkirk

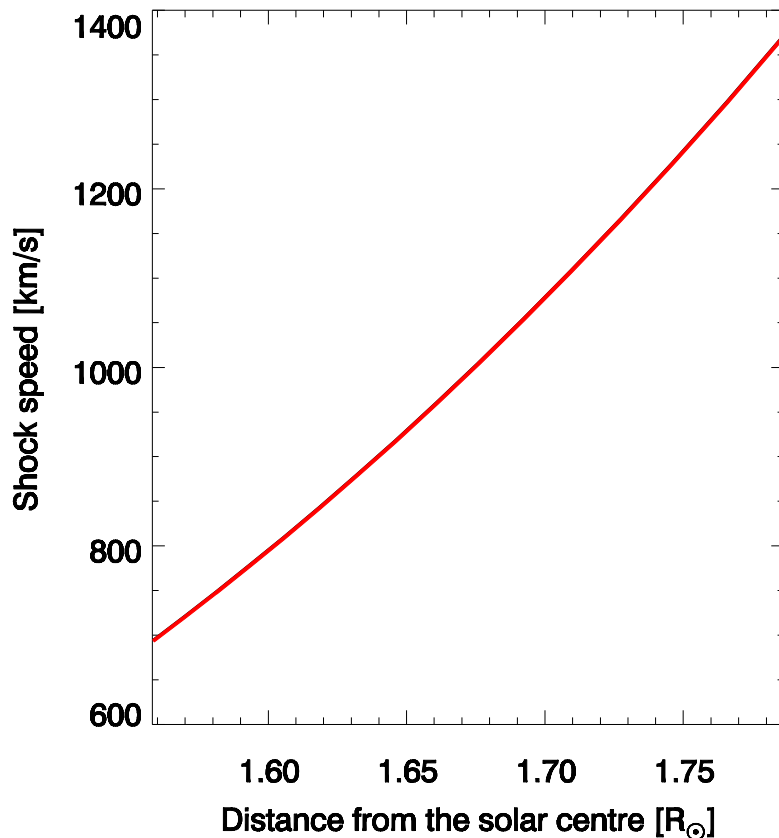
R = distance from solar centre [R_\odot]

- Can estimate the source's distance from the solar centre (R)
- R was estimated to be between 1.56-1.79 R_\odot



- Following calculations consider Upper Band frequency drift rate only
- The (radial) shock speed is calculated through:

$$V_{shock} = \frac{df_{pe}}{dt} \times \frac{2R_{\odot}n_e}{f_{pe}} \times \left(\frac{dn_e}{dR}\right)^{-1} \quad [\text{kms}^{-1}]$$



where: n_e = electron density [cm^{-3}]
 f = frequency [MHz]
 R = distance from solar centre [km]

- A band-splitting interpretation proposed by Smerd et al. (1974; 1975) attributes the splitting to *simultaneous emission from the upstream and downstream parts* of a shock front
- Relates band-splitting to the *Rankine-Hugoniot jump conditions* across the shock
- Relative bandwidth (BWD) related to density jump across the shock (Priest, 2014):

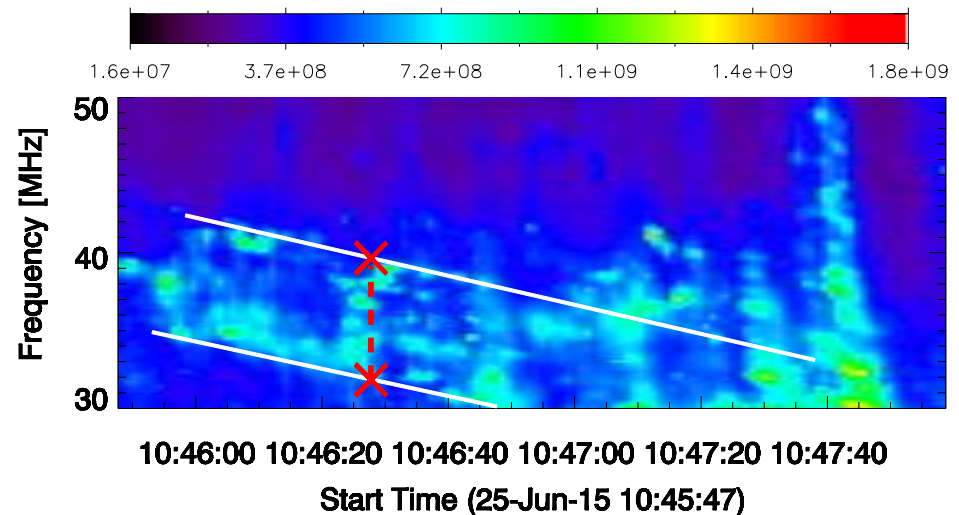
$$BWD = \frac{f_U - f_L}{f_L}$$

$$X \equiv \frac{n_2}{n_1} = \left(\frac{f_U}{f_L} \right)^2 = (BWD + 1)^2$$

where:

U = upper band (higher frequency)

L = lower band (lower frequency)



- Estimated (average) density jump, $X = 1.40$

- **Assume:** (i) plasma beta, $\beta = 0.5$
(ii) adiabatic index, $\gamma = 5/3$
(iii) angle between shock normal and upstream B-field, $\theta = 90^\circ$.

So, the Alfvén Mach Number, M_A (Vršnak et al., 2002):

$$M_A = \sqrt{\left(\frac{X(X + 5 + 5\beta)}{2(4 - X)}\right)}$$
$$= 1.55$$

And the Alfvén Speed, V_A :

$$V_A = \frac{V_{shock}}{M_A} \quad [kms^{-1}]$$

Since

$$V_A = \frac{B}{\sqrt{\mu_0 \rho}} = \frac{B}{\sqrt{4\pi \times 10^{-7} m_i n_i}} \quad [\text{ms}^{-1}]$$

Taking: $n_i = n_e$ and $m_i = m_{\text{proton}}$

The magnetic field is estimated using:

$$B_{\text{est}} = 5.1 \times 10^{-5} \times V_A \times f_{pe} \quad [\text{Gauss}]$$

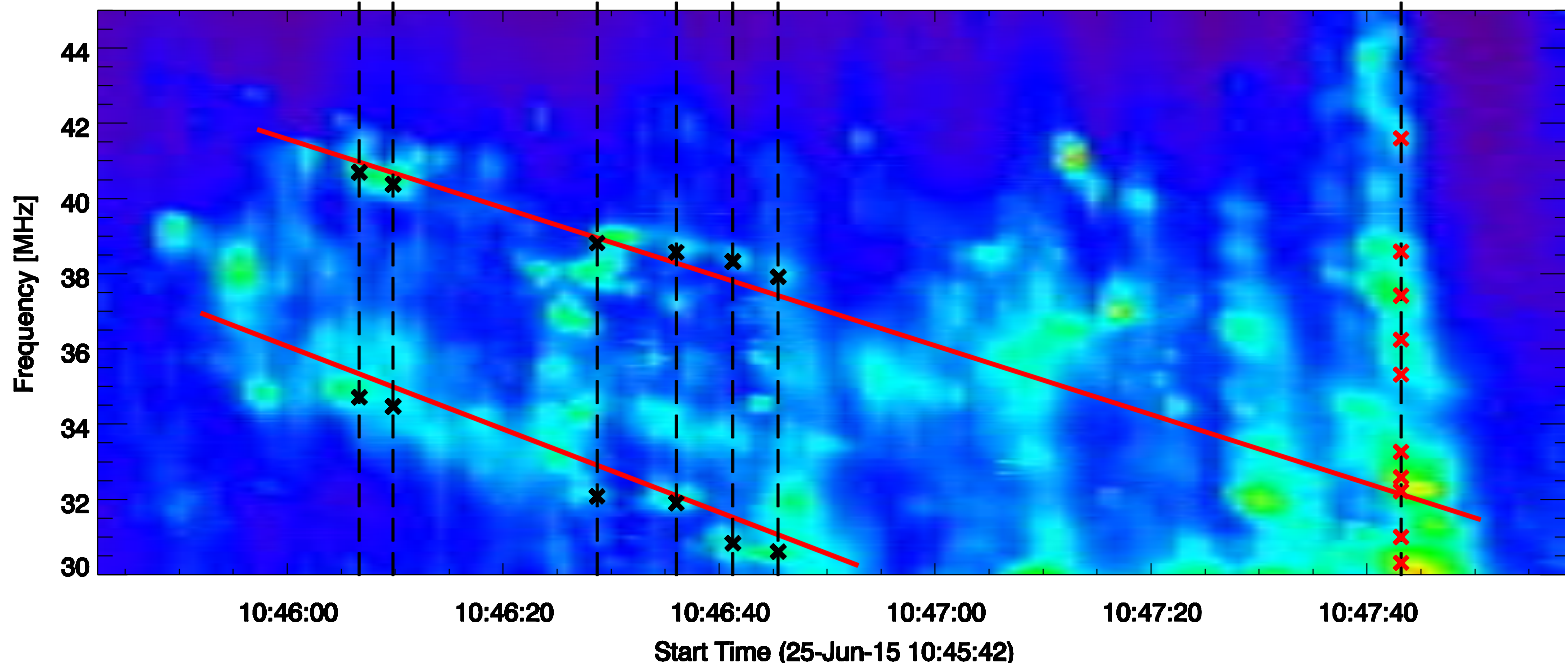
where: V_A is in kms^{-1}
 f_{pe} is in MHz

Compare to the magnetic field model e.g., Dulk and Mclean (1978):

$$B_{\text{model}} = 0.5(R - 1)^{-1.5} \quad [\text{Gauss}]$$

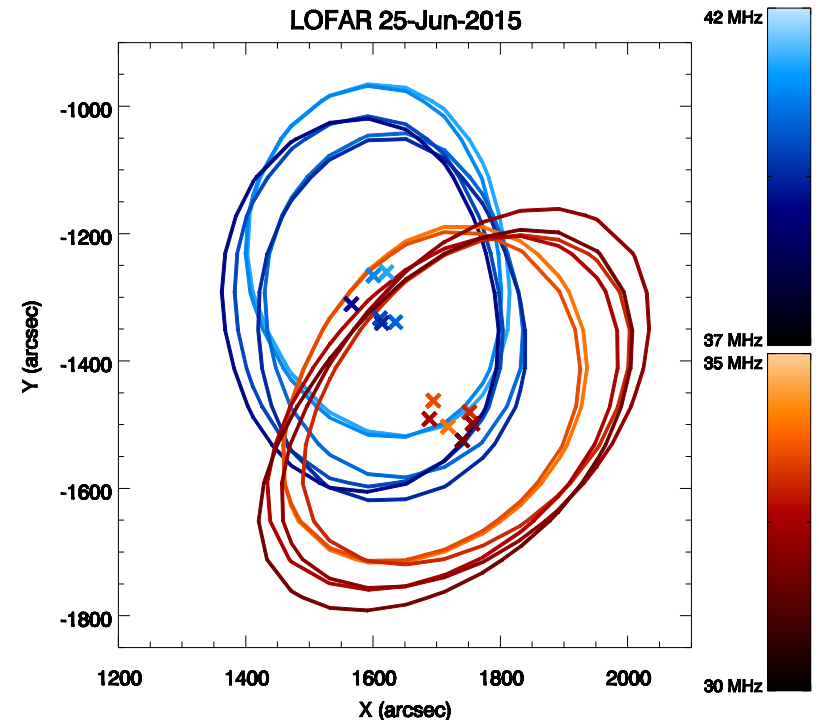
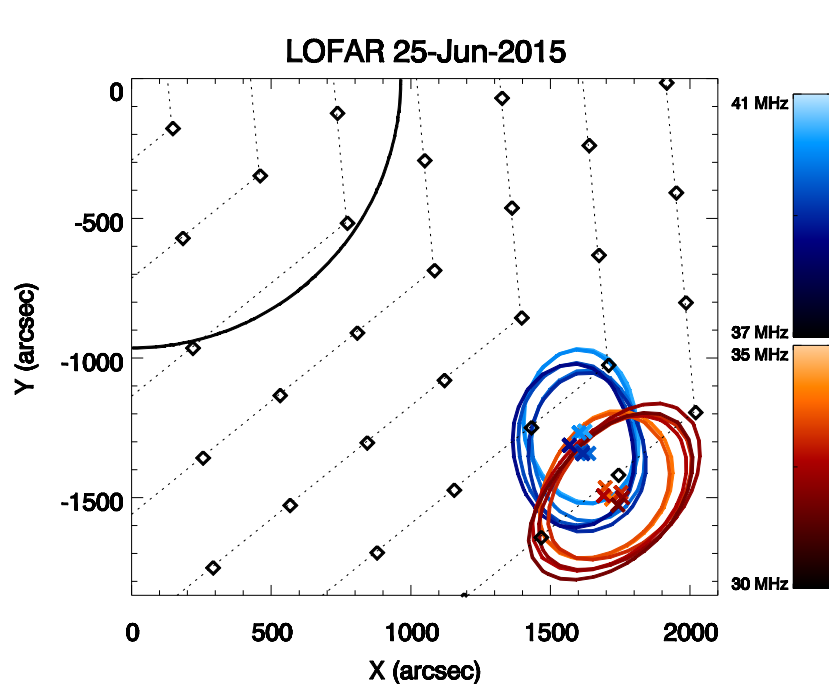
where: R = distance in R_{\odot}

- Imaging a specific moment in time and frequency enables the examination of the motion of the emission source during the observation
- Selected points in time and frequency for:
 - Type II* upper and lower bands (shown in black crosses)
 - Type III* burst at 10:47:43 UT (shown in red crosses)
- For the *Type II*: an UPPER band point and a LOWER band point is selected for each moment in time
- For the *Type III*: selected points across frequencies for a single moment in time



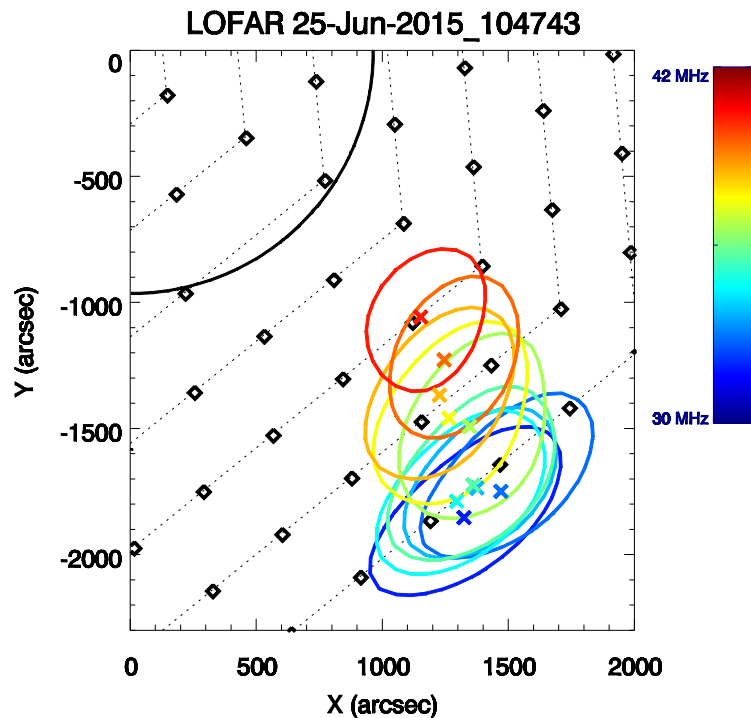
Type II:

- (left) Centroid locations plotted along with 90% maximum intensity contours for the Type II burst. The black diamonds represent individual beams and collectively the Field of View of LOFAR during the observation.
- (right) A magnification into the Type II sources and associated centroids
- Blue colour scheme used for **upper band** sources and red for the **lower band**.

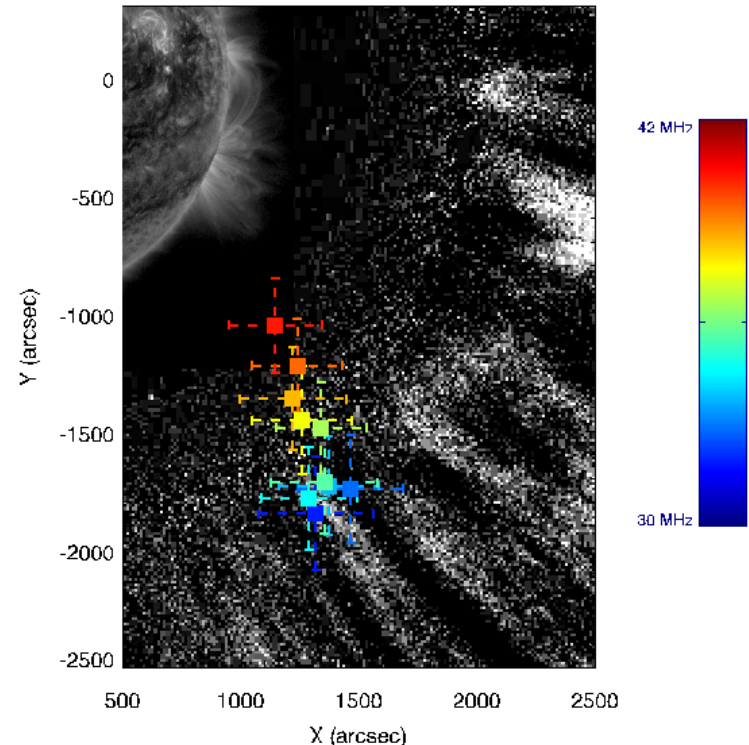


Type III:

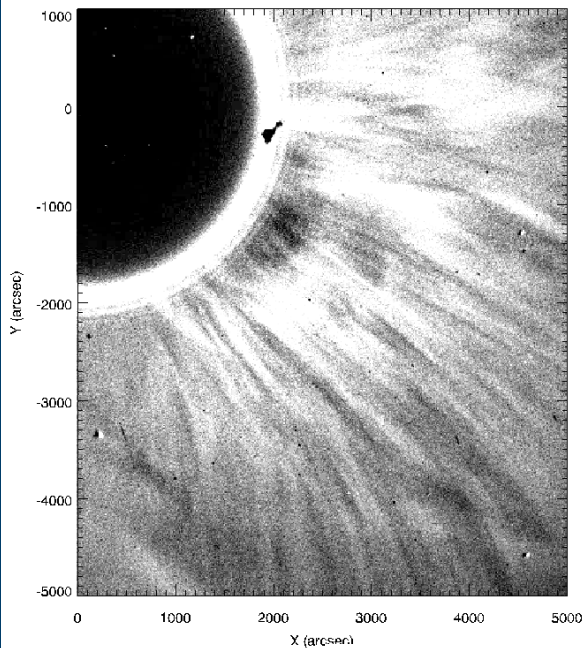
- (left) Centroid locations plotted along with 90% maximum intensity contours for the Type III burst. The black diamonds represent individual beams and collectively the Field of View of LOFAR during the observation.
- (right) Error bars assigned to Gaussian estimations of the Type III centroids



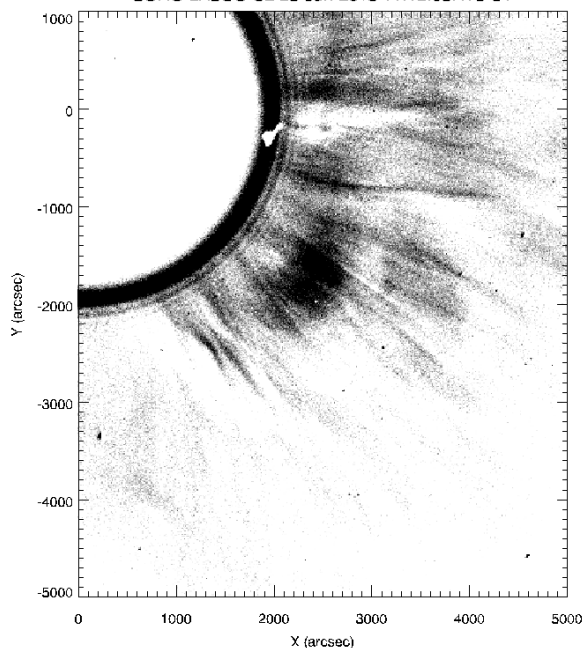
SOHO LASCO C2 25-Jun-2015 10:48:05.489 UT



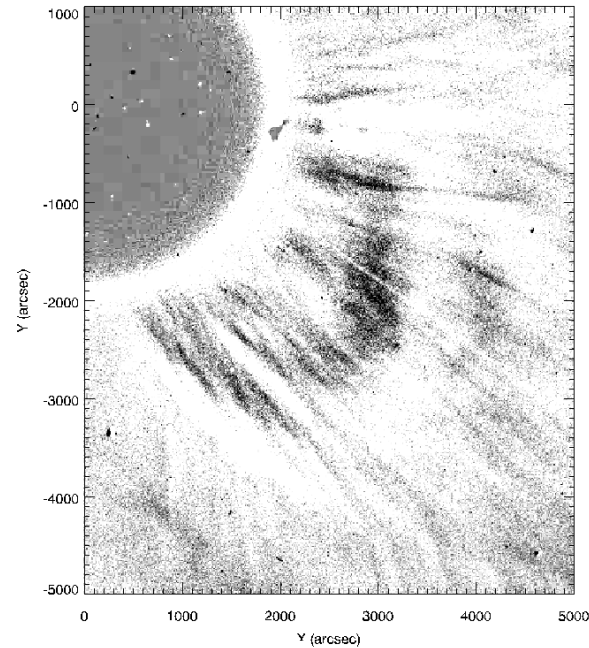
SOHO LASCO C2 25-Jun-2015 11:00:05.581 UT



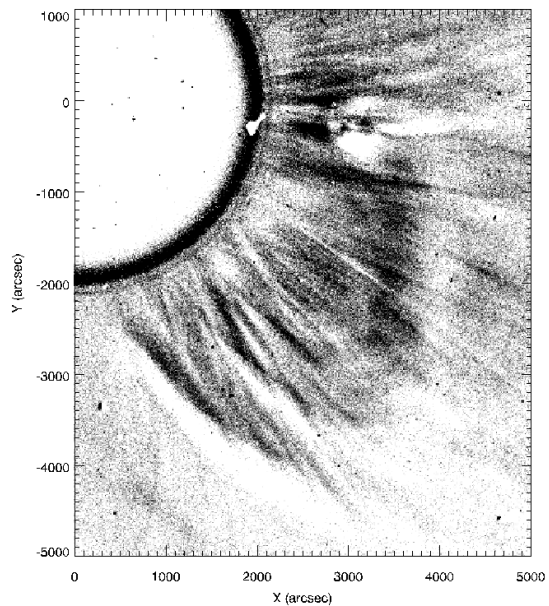
SOHO LASCO C2 25-Jun-2015 11:12:05.473 UT



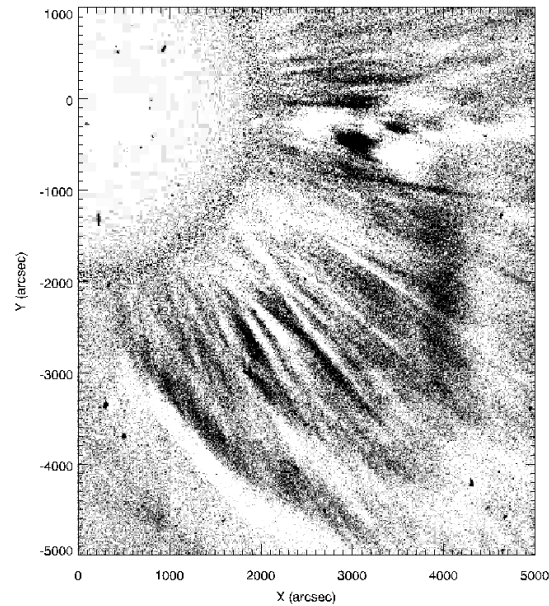
SOHO LASCO C2 25-Jun-2015 11:24:05.465 UT



SOHO LASCO C2 25-Jun-2015 11:36:05.456 UT

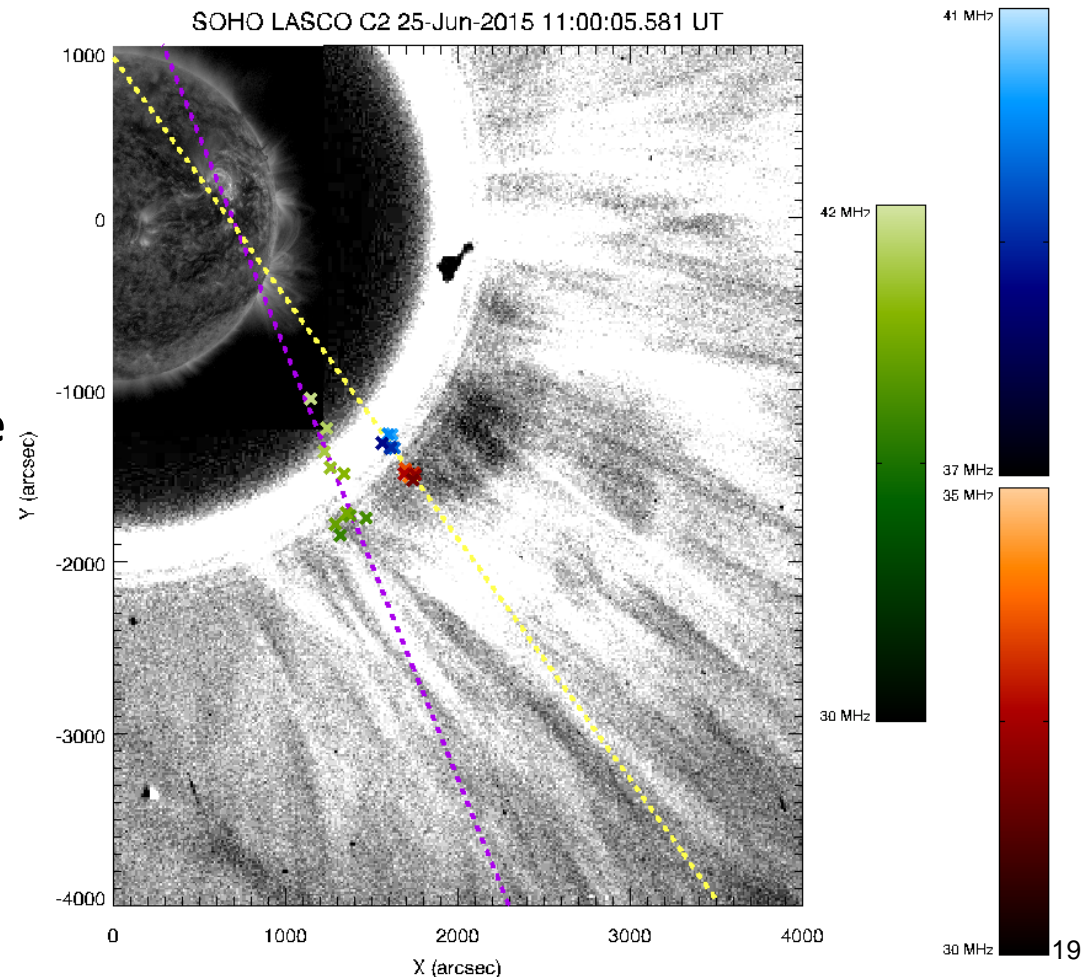


SOHO LASCO C2 25-Jun-2015 11:48:05.548 UT



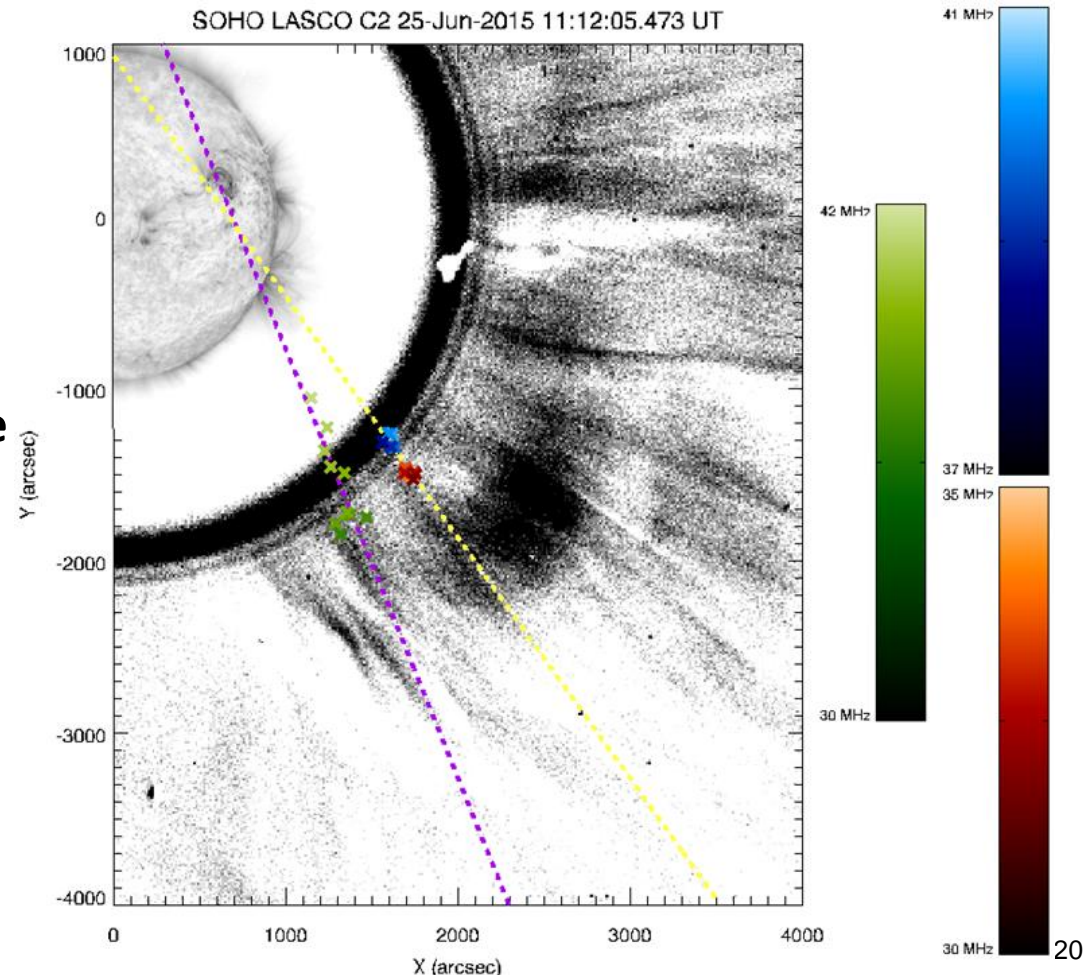
- **Combination of:**
 - SDO/AIA image showing solar surface near Type II occurrence time
 - SOHO/LASCO (C2) running difference image near Type II start time
 - Centroid locations obtained using LOFAR data

- **Crosses represent:**
 - Type II **upper band centroids**
 - Type II **lower band centroids**
 - Type III **centroids**
- **Fitted lines through both Type II (yellow) and Type III (purple) centroids point towards active region from which a CME at around 9:00 UT originated, but their location and timing coincides with the eruption at around 10:48 UT**



- **Combination of:**
 - SDO/AIA image showing solar surface near Type II occurrence time
 - SOHO/LASCO (C2) running difference image near Type II start time
 - Centroid locations obtained using LOFAR data

- **Crosses represent:**
 - Type II **upper band centroids**
 - Type II **lower band centroids**
 - Type III **centroids**
- **Fitted lines through both Type II (yellow) and Type III (purple) centroids point towards active region from which a CME at around 9:00 UT originated, but their location and timing coincides with the eruption at around 10:48 UT**



- 1. Relation of the morphological characteristics of dynamic spectra to parameters describing the local coronal environment and the shock wave properties, e.g.:**
 - Shock speed
 - Alfvén speed
 - Magnetic Field

- 2. Study of the Emission Source Motion**
 - Compared position of Type II upper and lower band sources
 - Compared position of Type II sources and Type III
 - Illustrated direction of propagation with respect to solar surface
 - Illustrated emission source locations with respect to solar eruptions

- 3. Objective: Compare observational results against band-splitting models (see e.g. Zimovets et al., 2012)**

THANK YOU

ANY QUESTIONS?

References:

- Dulk, G. A., & McLean, D. J. 1978, Sol. Phys., 57, 279
- McLean, D. J., & Labrum, N. R. 1985, Solar Radiophysics, CUP
- Newkirk, J. G. 1961, ApJ, 133, 983
- Priest, E. 2004, Magnetohydrodynamics of the Sun, CUP
- Smerd, S. F. et al. 1974, IAUS, 57, 389
- Smerd, S. F. et al. 1975, ApL, 16, 23
- Vršnak, B. et al. 2002, A&A, 396, 673
- White, S. M. 2007, Asian J. Phys., 16, 189
- Zimovets, I. et al. 2012, A&A, 547, A6